

## Wide speed range estimation using fuzzy logic controller for sensorless induction motor drives

Syed Sarver Maqdoom \*

PG student, EEE Department,  
Nimra college of engg & tech,  
Vijayawada, AP, INDIA.

Abdul Ahad Shaik\*\*

Associate professor & Head, EEE dept,  
Nimra college of engg & tech,  
Vijayawada, AP, INDIA,

**Abstract**—Recently, the development of speed estimation methods for sensorless control of induction motor drives has found great interest in the research community. Parameter adaptation schemes play an important role for better speed estimation over a wide range from zero to high levels beyond the rated speed. Therefore, parallel identification schemes for both speed and stator resistance of sensorless induction motor drives are proposed for a wide range of speed estimation. These estimation algorithms combine a sliding-mode current observer with Popov's hyper stability theory. Low- and zero-speed operations of the proposed sliding mode- observer (SMO)-based speed estimation combined with an online stator resistance adaptation scheme are investigated.

Fuzzy logic controllers (FLC's) have the following advantages over the conventional controllers: they are cheaper to develop, they cover a wider range of operating conditions, and they are more readily customizable in natural language terms.

### I. INTRODUCTION

Several methods have been recently proposed for speed estimation of sensorless induction motor drives [1], [2]. They can be classified into two major categories. The first one includes the techniques that estimate the rotor speed based on non ideal phenomena such as rotor slot harmonics and high frequency signal injection methods [3]. Such methods require spectrum analysis which, besides being time-consuming procedures, allow a narrow band of speed control. The second category of speed estimation methods relies on the model of the induction motor. The supremacy of a certain method depends on its estimation accuracy over a wide speed range. Model based methods of speed estimation are characterized by their simplicity, but sensitivity to parameter variations is considered the major problem associated with them. Stator resistance plays an important role, and its value has to be known with good precision in order to obtain accurate speed estimation in the low-speed region [4]. The interest in stator resistance adaptation came on the scene much recently, with the

advances of speed sensorless systems. It has also received more attention with the introduction of the direct torque control technique. An accurate value of the stator resistance is of crucial importance for the correct operation of a sensorless drive in the low-speed region, since any mismatch between the actual value and the set value used within the model of speed estimation may lead not only to a substantial speed estimation error but also to instability [5]–[7]. Therefore, there is a great interest in the research community to develop stator resistance identification schemes for accurate low-speed estimation. An offline estimation procedure of the motor parameters at various operating conditions is introduced in [7]. In that work, the stator resistance is observed to be varying as a function of stator temperature. The rotor resistance is also estimated offline for rotor field orientation as a function of slip frequency and rotor temperature. Numerous online estimation techniques are also proposed for continuously updating parameter values. An online rotor resistance estimation for rotor field orientation using a sliding mode observer (SMO) and a model reference adaptive system (MRAS) is proposed in [8]–[10]. The online stator resistance identification schemes can be classified into a couple of distinct categories. These schemes rely on stator current measurement and mostly require information regarding stator voltages [11]– [15]. The first category includes different types of estimators which often use an adaptive mechanism to update the value of stator resistance [11]– [14]. The stator resistance is determined in [11] by using a reactive-power-based MRAS. The reactive power relies on the accuracy of other parameters, such as leakage inductance and rotor resistance, which are not necessarily constant, and the result is prone to error. Adaptive full-order flux observers (AFFOs) for estimating the speed and stator resistance are developed using Lyapunov's stability criterion [12], [13]. While these schemes are not computationally intensive, an AFFO with a nonzero gain matrix may become unstable. An MRAS for estimating the speed and stator resistance is developed using Popov's stability criterion [14], [15]. Recently, two extended Kalman filter (EKF) algorithms for estimating stator and rotor resistances are utilized in a braided manner, thus achieving an accurate

estimation of a high number of parameters and states than would have been possible with a single EKF algorithm [16]. The second category of online stator resistance identification schemes depends on artificial intelligence techniques in the process of stator resistance adaptation. Artificial neural networks for estimating stator and rotor resistances are used for this purpose [17]. High-performance applications of sensorless systems require high accuracy of speed estimation over a wide speed range extending from very low and zero-speed operations to high speeds beyond the rating. Operation of field-oriented induction motors below the base speed is usually achieved with constant flux. Therefore, magnetizing inductance can be regarded as constant and equal to its rated value. In the field-weakening region, the rotor flux reference has to be reduced below its rated value. Variation of the rotor flux reference implies variable level of saturation, and consequently, magnetizing inductance of the machine is varied [18], [19]. Accurate value of magnetizing inductance is of utmost importance for many reasons. The first one is the correct setting of the *d*-axis stator current reference in a vector-controlled drive. The second one is its importance for accurate speed estimation in the field-weakening region, using machine-model-based approaches, of sensorless systems. The third reason is the dependency of rotor time constant identification schemes on magnetizing inductance, such as the method [22] utilizing reactive power. The accurate estimation of rotor time constant in the field-weakening region requires a correct value of the magnetizing inductance to be known.

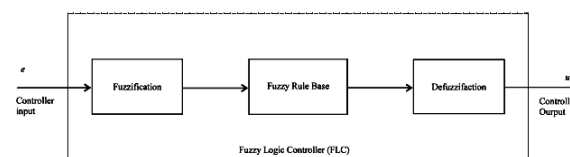
Several research and industrial applications concentrated their efforts on providing simple and easy control algorithms to cope with the increasing complexity of the controlled processes/systems [1]. The design method for a controller should enable full flexibility in the modification of the control surface [2]. The systems involved in practice are, in general, complex and time variant, with delays and nonlinearities, and often with poorly defined dynamics. Consequently, conventional control methodologies based on linear system theory have to simplify/linearize the nonlinear systems before they can be used, but without any guarantee of providing good performance. To control nonlinear systems satisfactorily, nonlinear controllers are often developed. The main difficulty in designing nonlinear controllers is the lack of a general structure [3]. In addition, most linear and nonlinear control solutions developed during the last three decades have been based on precise mathematical models of the systems. Most of those systems are difficult/impossible to be described by conventional mathematical relations, hence, these model-based

design approaches may not provide satisfactory solutions [4]. This motivates the interest in using FLC; FLCs are based on fuzzy logic theory [5] and employ a mode of approximate reasoning that resembles the decision making process of humans. The behavior of a FLC is easily understood by a human expert, as knowledge is expressed by means of intuitive, linguistic rules.

The block diagram of the generalized indistinct controller consists of four elements [13]:

- 1) 1 Fuzzification block, transforming input physical values  $y_i$  into corresponding linguistic variables  $\mu (y_i)$ ;
- 2) Knowledge base, containing rules table for logic output block;
- 3) Logic output block, transforming input linguistic variables into output with some belonging functions  $Con$ ;
- 4) Defuzzification block, transforming output linguistic variables into physical control influence.

Shows the structure of P-type a fuzzy controller. In this case, the error of regulation  $\epsilon$  may be taken as the input information. The output information is the signal of the relative duration of conducting state of the switch  $Con = tk/T - (k-1)$ . The structure of PI Fuzzy controller is shown in. The input variables of this controller are, accordingly, the error of regulation  $\epsilon$  and its derivative  $\dot{\epsilon}$ . The output is the gain.

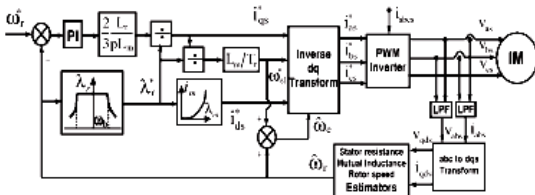


General structure of a fuzzy logic controller

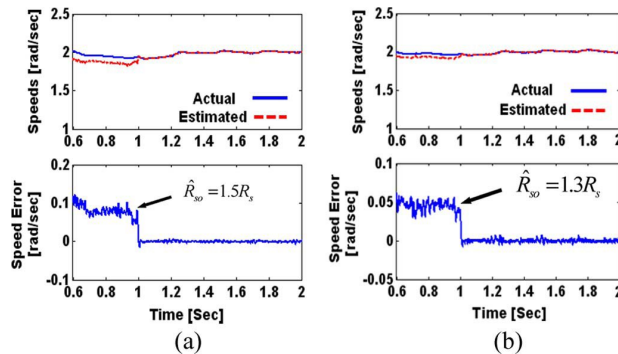
## II. SYSTEM IMPLEMENTATION

The basic configuration of the experimental system is shown in Fig. 4. It consists of an induction motor interfaced with a digital control board DS1102 based on a Texas Instruments TMS320C31 DSP for speed estimation. The induction motor is coupled with a dc generator for mechanical loading. The rating and parameters of the induction motor are given in the Appendix. Stator terminal voltages and currents are measured and filtered using analog circuitry. Hall-effect sensors are used for this purpose. The measured voltage and current signals are acquired by the A/D input ports of the DSP control board. This board is hosted by a

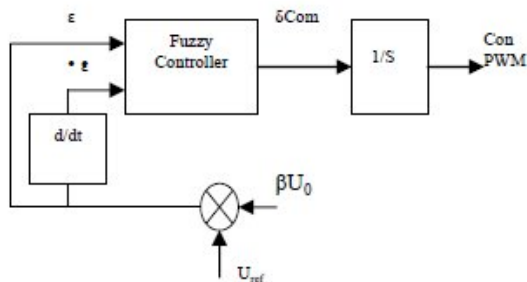
personal computer on which mathematical algorithms are programmed and downloaded to the board for real-time speed estimation. A direct speed measurement is also carried out for comparison with the estimated speed. The output switching commands of the DSP control board are obtained via its digital ports and interfaced with the inverter through opto isolated gate drive circuits.



IFO controller with compensation of flux saturation.



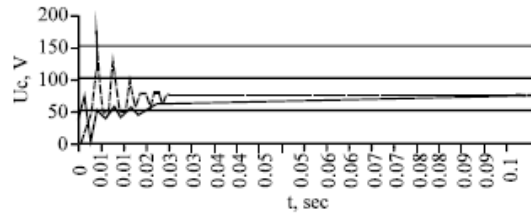
Actual and estimated speeds, and speed estimation error at speed command of 2 rad/s. Stator resistance adaptation is activated at  $t = 1$ s. (a)  $\hat{R}_{so} = 1.5 R_s$ . (b)  $\hat{R}_{so} = 1.3 R_s$ .



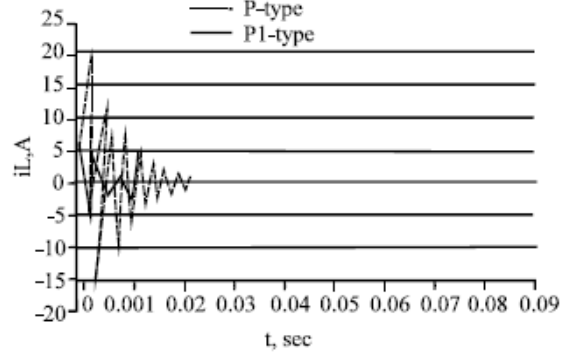
Block diagram of PI-type fuzzy controller

**Comparison for quality parameters of PI and Fuzzy controllers:** The following values were taken for comparison:  $U_{ref} = 3$ ;  $\beta = 0,04$ ,  $kU_{in}$ : 0,25; 0,5; 1,0; 2,0; 4,0; 0: 0,1; 0,2; 0,3. The Simulation of the structure of fig. 4 allows defining the value of the static regulation error  $\epsilon$  and the values of overcorrection 8. For that, it was necessary to vary the parameters of an input voltage

in the above-mentioned range and the factor of error scaling  $kU_{in}$ . The results given in tables 3, 4 are obtained at a value of loading resistance  $R_0 = 300$  Ohm. It is found that with the increasing of error scaling factor  $kU_{in}$ , the static error is decreased and the overregulation is increased. The value of static error was defined for the input voltage  $U_{in} = 60$  V only, quasiperiodic oscillations were observed for other values of the input voltage. The estimation of the specified parameters of the controller structure of Fig. 7 isn't given, as it is practically static ( $\approx 0,1\%$ ) with a periodic transient.

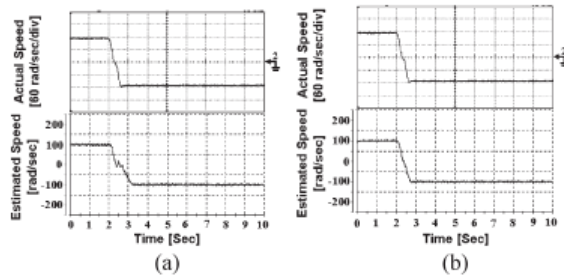


Time-domain transient of the input current



A sensorless indirect field-oriented (IFO) controlled induction motor drive, shown in Fig. 5, is used, where the actual speed feedback signal is replaced by the estimated one. The sensitivity to stator resistance mismatch is shown in Fig. 6 for +20%  $R_s$  error at high and low speeds. These results show that the speed estimation error at high-speed operation (150 rad/s) is 1.9 rad/s (1.26%), and that at low-speed operation (3 rad/s) is 0.32 rad/s (10.7%). Large error at low speeds may cause instability. In order to avoid this, the online stator resistance adaptation scheme (22) has been applied. The initial detuning in the stator resistance takes values of  $-10\%$  and  $-50\%$ , as shown in Fig. 7(a). In both cases, the stator resistance adaptation was activated at  $t = 0$ . It is clear that the stator resistance estimator quickly removes the initial stator resistance error and consequently eliminates the large speed estimation error. A considerable reduction of the speed error is observed with stator resistance adaptation due to  $-50\%$  initial  $R_s$  mismatch in the observer, as shown in Fig. 7(b).

Since motor heating usually causes a considerable variation in the winding resistance, so there is often a mismatch between the actual stator resistance and its corresponding set value within the model used for speed estimation. For this purpose, the proposed SMO with a stator resistance identification scheme is first tested under different values of stator resistance to represent this parameter mismatch. Fig. 13 shows the estimated speed at 10 rad/s at +50% stator resistance mismatch with activated stator resistance adaptation. It is observed that the estimated speed preserves its value unchanged under this parameter mismatch. This test proves that the proposed SMO with online stator resistance tuning is dependable and accurately gives the same behavior as the actual speed under stator resistance mismatch.



Actual and estimated speeds during speed reversal at 100 rad/s (a) without stator resistance adaptation and (b) with stator resistance adaptation.

IV CONCLUSION

In this paper, parallel speed and stator resistance identification schemes of sensorless induction motor drives have been introduced to overcome the problem of resistance variation. Estimation algorithms have been obtained based on a sliding mode current observer combined with Popov’s hyper stability theory. It has been found that activation of the stator resistance adaptation mechanism quickly compensates the initial error in the estimated stator resistance value and therefore eliminates the initial speed estimation error. As a consequence, the actual and estimated speeds become in very good agreement. Low and zero-speed sensorless operations have also been investigated by the proposed SMO combined with the online stator resistance adaptation scheme.

Fuzzy logic provides a certain level of artificial intelligence to the conventional controllers, leading to the effective fuzzy controllers. Process loops that can benefit from a non-linear control response are excellent candidates for fuzzy control. Since fuzzy logic provides fast response times with virtually no overshoot. Loops

with noisy process signals have better stability and tighter control when fuzzy logic control is applied.

P Fuzzy controller has smaller sensitivity to the change in the input voltage, however, more sensitivity is observed to load changes. PI- Fuzzy controller has less sensitivity to load changes, where, higher sensitivity to the change of the input voltage is observed.

Analysis of transient and static error of regulation has shown advantage of an indistinct PI-controller for the output voltage over the P-type fuzzy controller.

P Fuzzy controller has faster transient as compared to PI controller, while, transient for PI Fuzzy controller is almost periodic.

IV APPENDIX

A. List of Symbols

- $L_m$  Magnetizing inductance.
- $L_s, L_r$  Stator and rotor leakage inductances.
- $R_s$  Stator resistance.
- $T_r$  Rotor time constant.
- $\omega_r, \hat{\omega}_r$  Actual and estimated rotor speeds.
- $\sigma$  Leakage coefficient.
- $\hat{i}_s^* = [\hat{i}_{ds}^* \hat{i}_{qs}^*]^T; \hat{i}_r^* = [\hat{i}_{dr}^* \hat{i}_{qr}^*]^T$  Actual and estimated stator current vectors.

- $\lambda_r^* = [\lambda_{dr}^* \lambda_{qr}^*]^T; \hat{\lambda}_r^* = [\hat{\lambda}_{dr}^* \hat{\lambda}_{qr}^*]^T$  Actual and estimated rotor flux vectors.
- $v_s^* = [v_{ds}^* v_{qs}^*]^T$  Stator voltage vector.

$$A_{11} = aI \quad A_{12} = cI + dJ \quad A_{21} = eI$$

$$A_{22} = -\varepsilon A_{12} \quad b_1 = bI$$

$$I = \begin{bmatrix} 1 & 0 \\ 0 & 1 \end{bmatrix} \quad J = \begin{bmatrix} 0 & -1 \\ 1 & 0 \end{bmatrix}$$

$$a = -\left(\frac{R_s}{\sigma L_s} + \frac{L_m^2}{\sigma L_s T_r L_r}\right)$$

$$c = \frac{1}{\varepsilon T_r} \quad d = \frac{\omega_r}{\varepsilon} \quad e = \frac{L_m}{T_r}$$

$$\varepsilon = \frac{\sigma L_s L_r}{L_m} \quad b = \frac{1}{\sigma L_s} \quad \sigma = 1 - \frac{L_m^2}{L_s L_r} \quad T_r = \frac{L_r}{R_r}$$

B. Induction Motor Parameters

Table I

INDUCTION MOTOR PARAMETERS

|                      |     |             |        |
|----------------------|-----|-------------|--------|
| Rated power (w)      | 250 | $R_s$ (p.u) | 0.0658 |
| Rated voltage (volt) | 250 | $R_s$ (p.u) | 0.0658 |
| Rated current (Amp)  | 250 | $R_s$ (p.u) | 0.0658 |
| Rated frequency (Hz) | 250 | $R_s$ (p.u) | 0.0658 |
| Number of poles      | 250 | $R_s$ (p.u) | 0.0658 |

IV REFERENCES

- [1] Wide-Speed-Range Estimation with Online Parameter Identification Schemes of Sensorless Induction Motor Drives Mohamed S. Zaky, Mahmoud M. Khater, Shokry S. Shokralla, and Hussain A. Yasin.
- [2] M. S. Zaky, M. M. Khater, H. Yasin, S. S. Shokralla, and A. El-Sabbe, "Speed-sensorless control of induction motor drives," *Eng. Res. J.*, vol. 30, no. 4, pp. 433–444, Oct. 2007.
- [3] Q. Gao, G. Asher, and M. Sumner, "Sensorless position and speed control of induction motors using high-frequency injection and without offline precommissioning," *IEEE Trans. Ind. Electron.*, vol. 54, no. 5, pp. 2474–2481, Oct. 2007.
- [4] H. Tajima, G. Guidi, and H. Umida, "Consideration about problems and solutions of speed estimation method and parameter tuning for speed sensorless vector control of induction motor drives," *IEEE Trans. Ind. Appl.*, vol. 38, no. 5, pp. 1282–1289, Sep./Oct. 2002.
- [5] J. Holtz and J. Quan, "Sensorless vector control of induction motors at very low speed using a nonlinear inverter model and parameter identification," *IEEE Trans. Ind. Appl.*, vol. 38, no. 4, pp. 1087–1095, Jul./Aug. 2002.
- [6] G. Guidi and H. Umida, "A novel stator resistance estimation method for speed-sensorless induction motor drives," *IEEE Trans. Ind. Appl.*, vol. 36, no. 6, pp. 1619–1627, Nov./Dec. 2000.
- [7] Verbruggen, H. B. and Bruijn, P. M., 1997. Fuzzy control and conventional control: What is (And Can Be) the Real Contribution of Fuzzy Systems *Fuzzy Sets Systems, Vol. 90*, 151–160.
- [8] Kowalska, T. O., Szabat, K. and Jaszczak, K., 2002. The Influence of Parameters and Structure of PI-Type Fuzzy-Logic Controller on DC Drive System Dynamics, *Fuzzy Sets and Systems, Vol. 131*, 251-264.
- [9] Ahmed, M. S., Bhatti, U. L., Al-Sunni, F. M. and El-Shafei, M., 2001. Design of a Fuzzy Servo-Controller, *Fuzzy Sets and Systems, vol. 124*: 231-247.
- [10] Zilouchian, A., Juliano, M., Healy, T., 2000. Design of Fuzzy Logic Controller for a Jet Engine Fuel System, *Control and Engineering Practices*, Vol. 8: 873-883.
- [11] Zadeh, L. A., 1965. Fuzzy sets, *Information Control*, Vol. 8, pp: 339-353.
- [13] Liu, B. D., 1997. Design and Implementation of the Tree-Based Fuzzy Logic Controller, *IEEE Transactions on Systems, Man, and Cybernetics*, Part B: Cybernetics., Vol.27, No.3, 475-487.